

Measurements of Baryon-Strangeness Correlations at RHIC

Toshihiro Nonaka (野中俊宏)
University of Tsukuba
PHD2024 @CCNU, Wuhan

Outline

- Introduction
- Analysis
- Results
- Summary



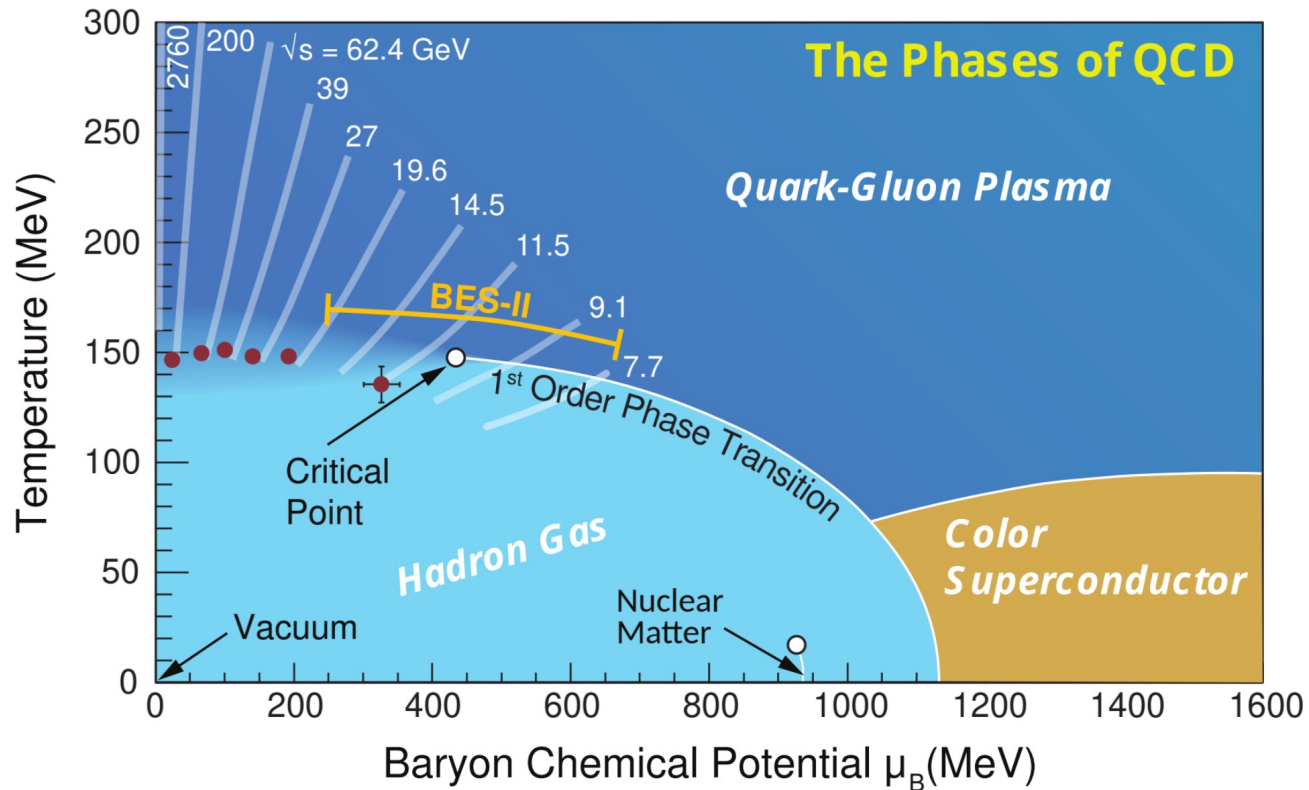
筑波大学
University of Tsukuba



筑波大学
宇宙史研究センター
Tomonaga Center for the History of the Universe

Introduction

“Conjectured” QCD phase diagram



A. Bzdak et al, *Phys.Rep.853 pp1-87 (2020)*

- Crossover at $\mu_B = 0$ MeV
 - Y. Aoki et al, *Nature* 443,675(2006)
- 1st-order phase transition at large μ_B ?
- Critical point?

Cumulants of conserved charges

- Measure event-by-event distributions of **net-baryon**, **net-charge**, and **net-strangeness** number

$$\Delta N_q = N_q - N_{\bar{q}}, \quad q = B, Q, S$$

(1) Sensitive to the correlation length

$$C_2 \approx \xi^2, C_3 \approx \xi^{4.5}, C_4 \approx \xi^7, C_5 \approx \xi^{9.5}, C_6 \approx \xi^{12}$$

M. A. Stephanov, PRL102.032301(2009), PRL107.052301(2011)
M. Asakawa, S. Ejiri, and M. Kitazawa, PRL103.262301(2009)

(2) Comparison with susceptibilities

$$S\sigma = \frac{C_3}{C_2} = \frac{\chi_3}{\chi_2} \quad \kappa\sigma^2 = \frac{C_4}{C_2} = \frac{\chi_4}{\chi_2}$$

$$\chi_n^q = \frac{1}{VT^3} \times C_n^q = \frac{\partial^n p/T^4}{\partial \mu_q^n}, \quad q = B, Q, S$$

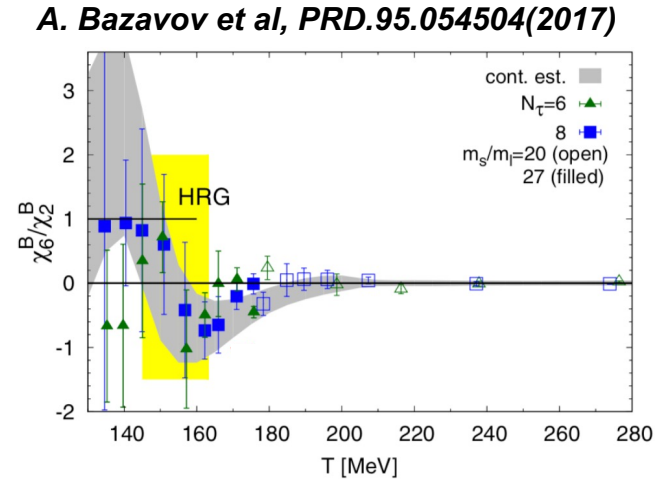
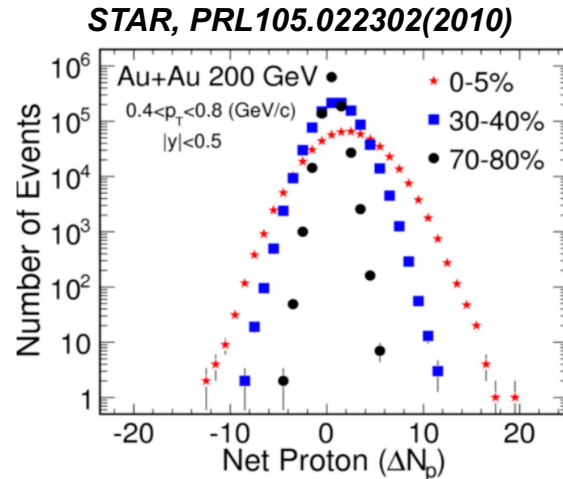
Cumulant ↔ Central moment

$$C_1 = \langle N \rangle, \quad C_2 = \langle (\delta N)^2 \rangle$$

$$C_3 = \langle (\delta N)^3 \rangle, \quad C_4 = \langle (\delta N)^4 \rangle - 3 \langle (\delta N)^2 \rangle^2$$

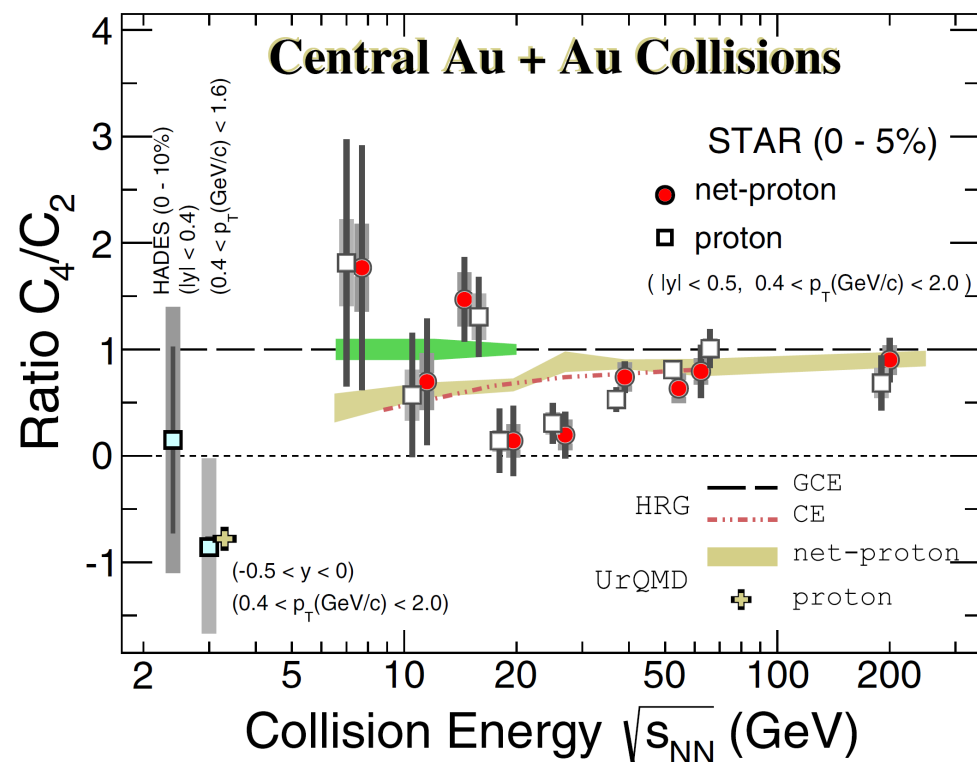
$$C_5 = \langle (\delta N)^5 \rangle - 10 \langle (\delta N)^2 \rangle \langle (\delta N)^3 \rangle$$

$$C_6 = \langle (\delta N)^6 \rangle + 30 \langle (\delta N)^2 \rangle^3 - 15 \langle (\delta N)^2 \rangle \langle (\delta N)^4 \rangle$$



Net-proton 4th-order cumulant

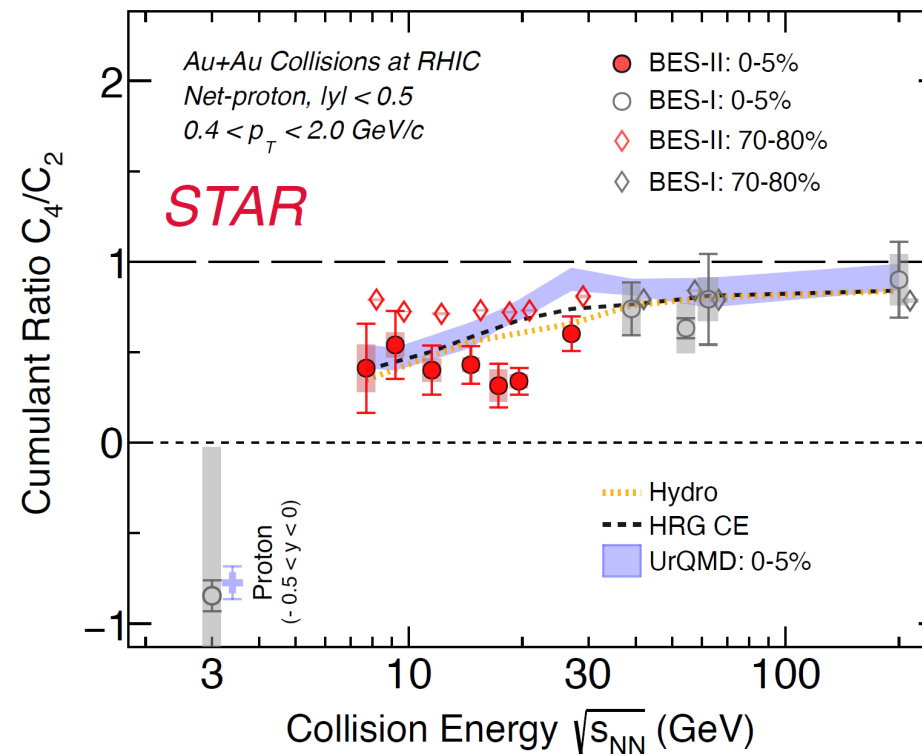
- Critical region at $\sqrt{s_{NN}} > 3$ GeV



HADES, PRC102.024914(2020)

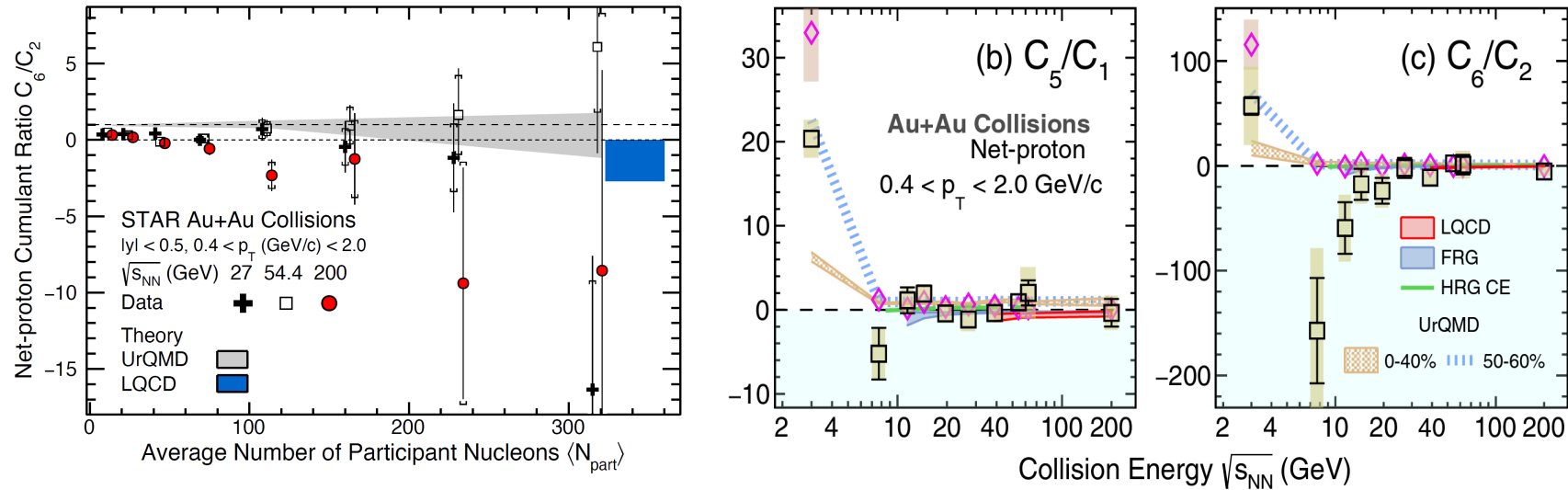
STAR, PRL128.202303(2022), PRC107.024908(2023)

- Suppression at $\sqrt{s_{NN}} \sim 20$ GeV

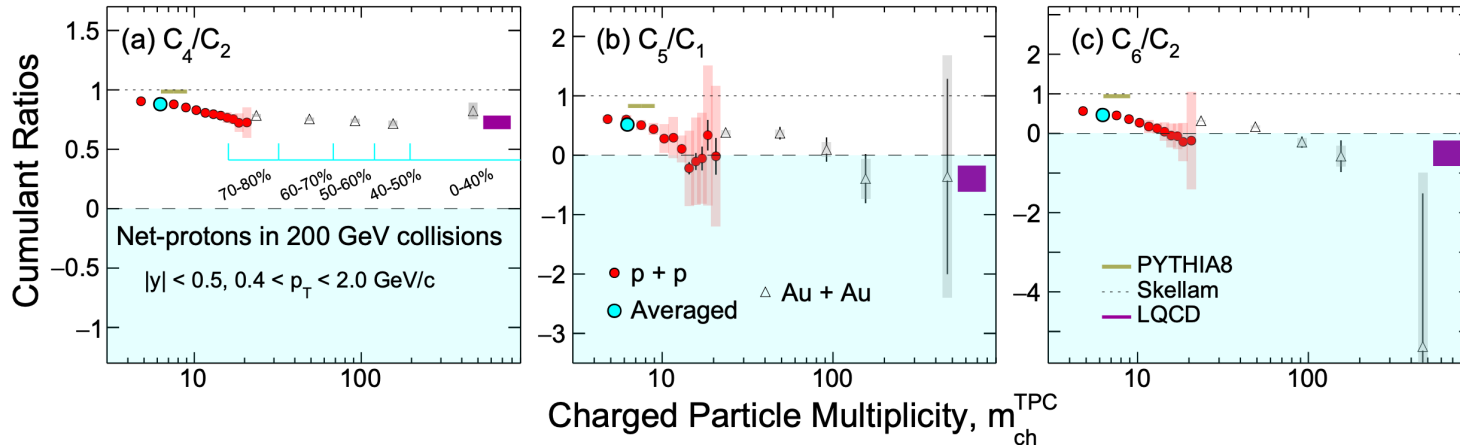


A. Pandav, CPOD2024

Net-proton hyper-order cumulants



STAR, PRL127.262301(2021)
STAR, PRL130.082301(2023)
STAR, PLB 857.138966(2024)

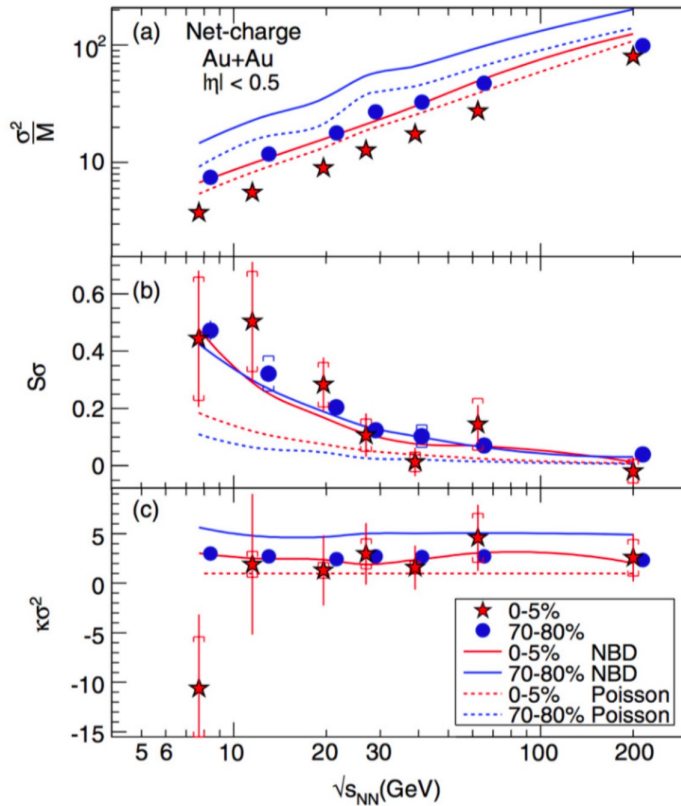


- Signature of a smooth crossover at $\mu_B=25$ MeV?
- Probing the phase boundary over wide μ_B region?
- QGP at the highest-multiplicity events at p+p 200 GeV collisions?

Net-charge, net-kaon cumulants

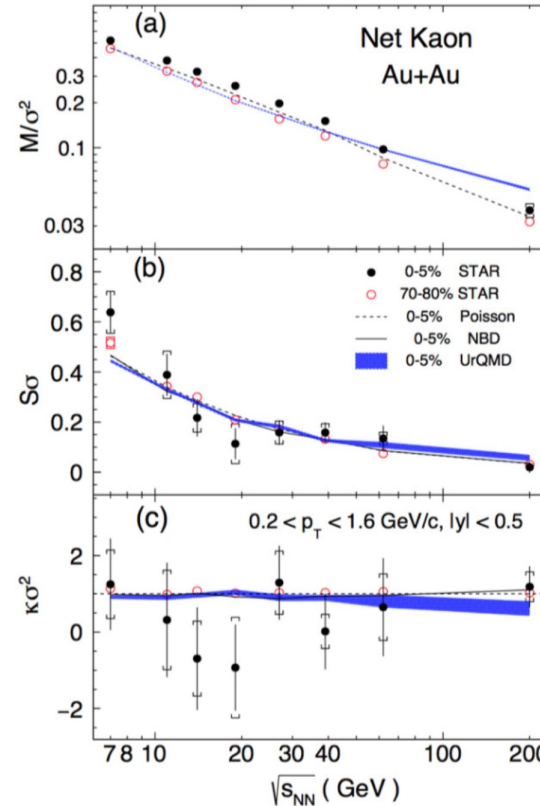
Net-charge

STAR: PRL113, 092301(2014)



Net-kaon

STAR: PLB, 785, 551(2018)

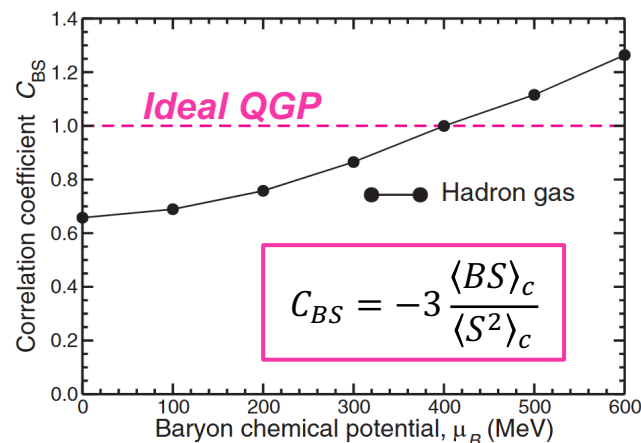


$$\text{error}(\kappa\sigma^2) \propto \frac{\sigma^2}{\varepsilon^2} \frac{1}{\sqrt{N_{\text{evts}}}}$$

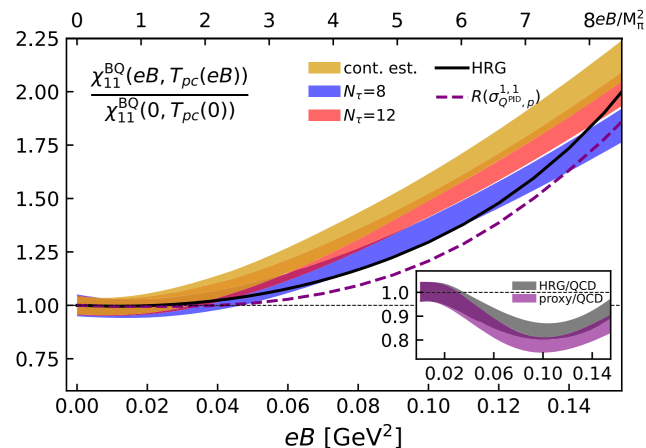
✓ Large statistical uncertainties, need more data.

Mix-cumulants

V. Koch et al, PRL95.182301(2005)

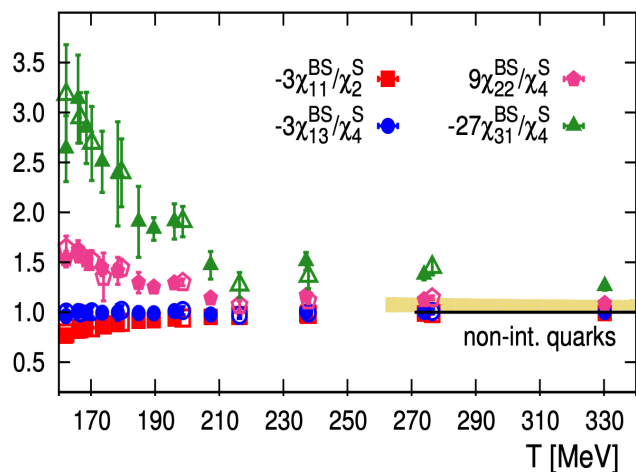


H-T.Ding et al, PRL132.201903(2024)

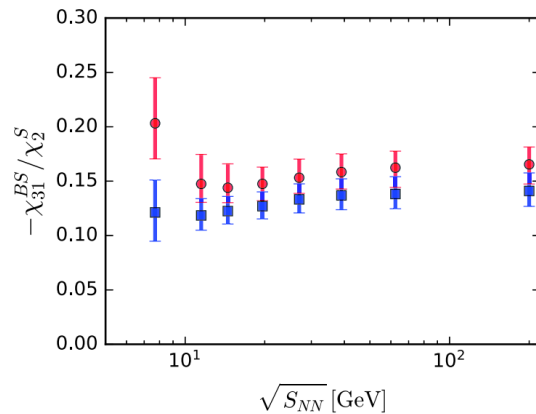


- Mix-cumulants among conserved charges are suggested to be sensitive to the magnetic field as well as QCD phase structure.
- This presentation focuses on baryon-strangeness correlations.

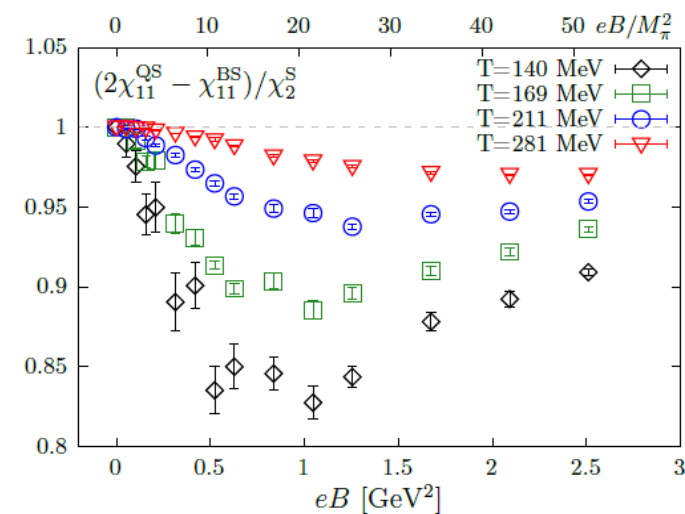
A. Bazavov et al, PRL111.082301(2013)



R. Wen and W.J. Fu, CPC45.044112(2021)



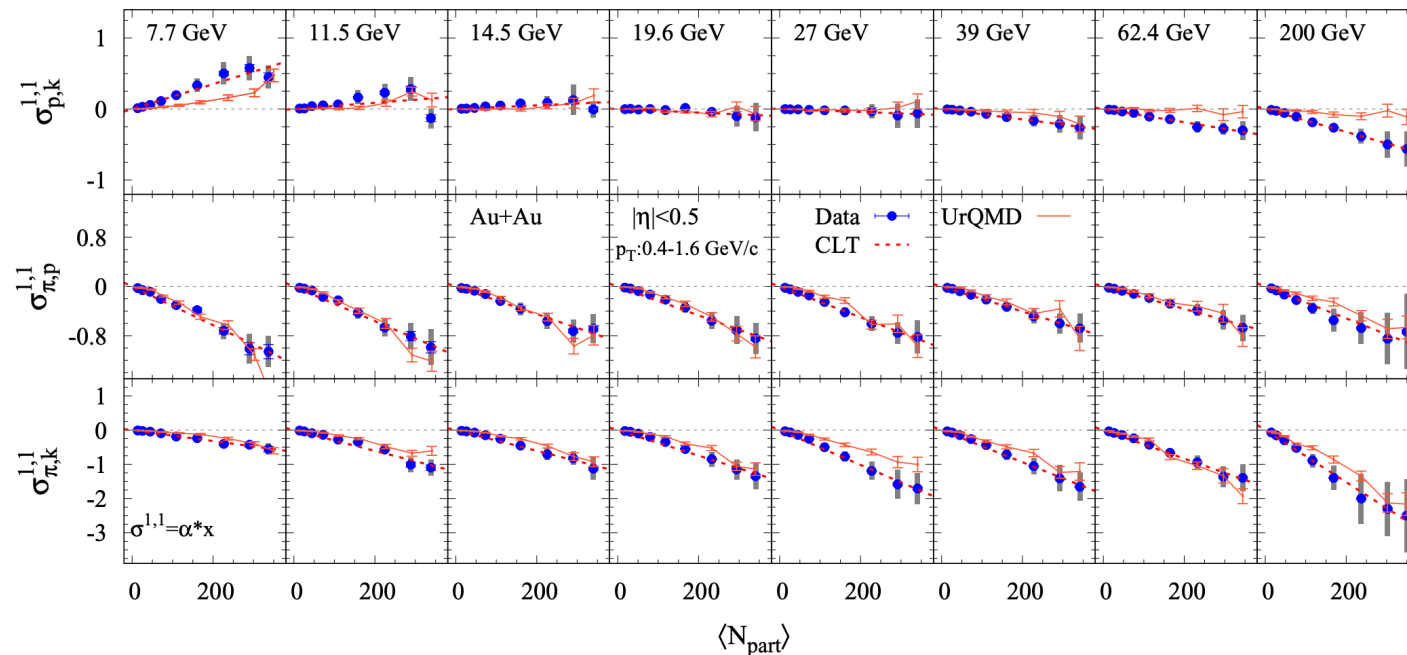
H-T.Ding et al, EPJA57.202(2021)



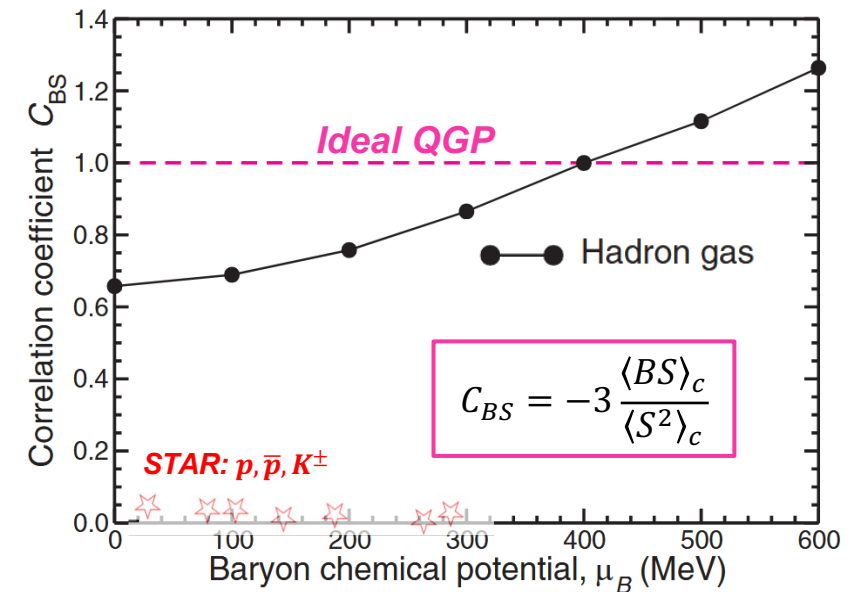
First measurement from RHIC

- Proton-kaon correlations are ~ 20 times smaller than the theoretical guidance on BS correlations.

STAR: PRC100,014902(2019), PRC105.029901(2022)

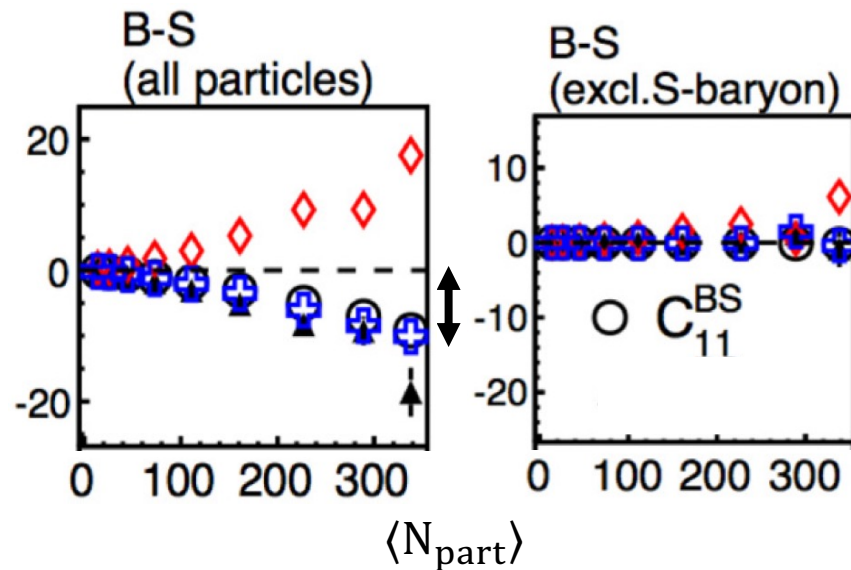


V. Koch et al, PRL95.182301(2005)



What was missing?

- Model studies indicate that the most of baryon-strangeness correlations are carried by hyperons.
- Measuring event-by-event fluctuations of hyperons is a key to improve the baryon-strangeness correlations.



UrQMD: Z. Yang et al, PRC95.014914(2017)

STAR: PRC100,014902(2019)

strange particles. It is difficult to perform high-purity event-by-event measurements of neutral strange baryons such as Λ , strange mesons such as K_S^0 or other heavy conserved charge-carrying particles such as Ω , Σ , Ξ , etc. This is because they require reconstruction using invariant mass spectra that reduces both the efficiency and purity of their detection [44].

Effect of hyperons

$$\langle XY \rangle_c = \langle XY \rangle - \langle X \rangle \langle Y \rangle$$

ΔX : net-particle number of specie X

p, pbar, K⁺, K⁻

$$\langle BS \rangle_c = \langle \Delta p \Delta K \rangle_c$$

- The effect is as large as the yields of hyperons.

↓ +Λ + Λ̄

p, pbar, K⁺, K⁻, Λ, Λ̄

$$\begin{aligned} \langle BS \rangle_c &= \langle (\Delta p + \Delta \Lambda)(\Delta K - \Delta \Lambda) \rangle_c \\ &= \langle \Delta p \Delta K \rangle_c - \langle \Delta p \Delta \Lambda \rangle_c + \langle \Delta \Lambda \Delta K \rangle_c - \langle \Delta \Lambda^2 \rangle_c \end{aligned}$$

Poisson

$$-(\langle \Lambda \rangle_c + \langle \bar{\Lambda} \rangle_c)$$

↓ +Ξ⁻ + Ξ̄⁺

p, pbar, K⁺, K⁻, Λ, Λ̄, Ξ⁻, Ξ̄⁺

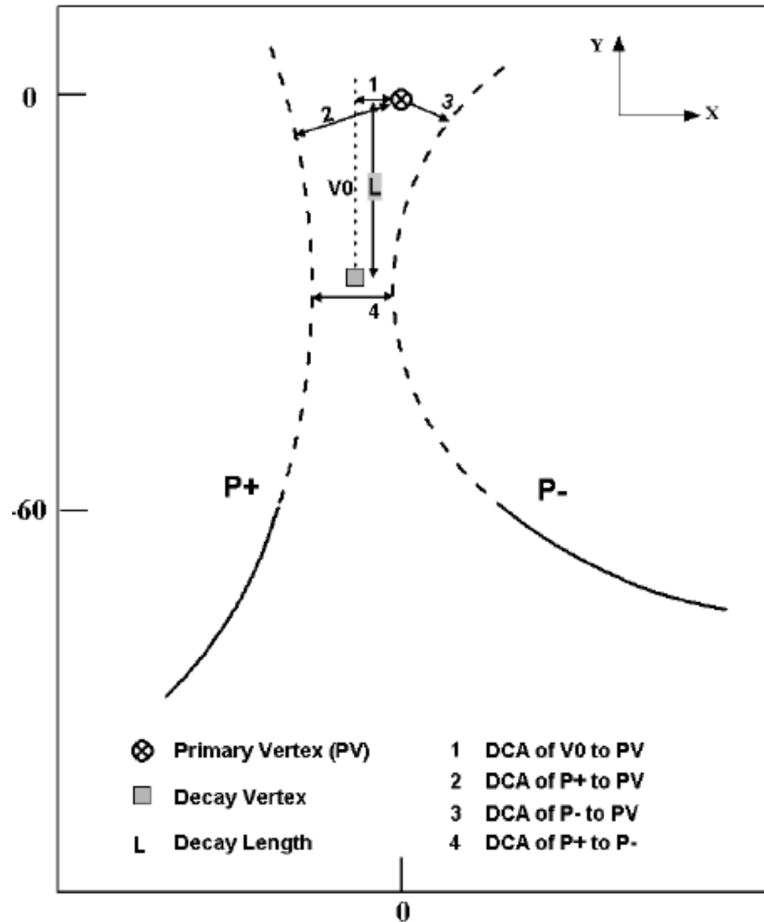
$$\begin{aligned} \langle BS \rangle_c &= \langle (\Delta p + \Delta \Lambda + \Delta \Xi)(\Delta K - \Delta \Lambda - 2\Delta \Xi) \rangle_c \\ &= \langle \Delta p \Delta K \rangle_c - \langle \Delta p \Delta \Lambda \rangle_c - 2\langle \Delta p \Delta \Xi \rangle_c + \langle \Delta \Lambda \Delta K \rangle_c - \langle \Delta \Lambda^2 \rangle_c \\ &\quad - 3\langle \Delta \Lambda \Delta \Xi \rangle_c + \langle \Delta \Xi \Delta K \rangle_c - 2\langle \Delta \Xi^2 \rangle_c \end{aligned}$$

Poisson

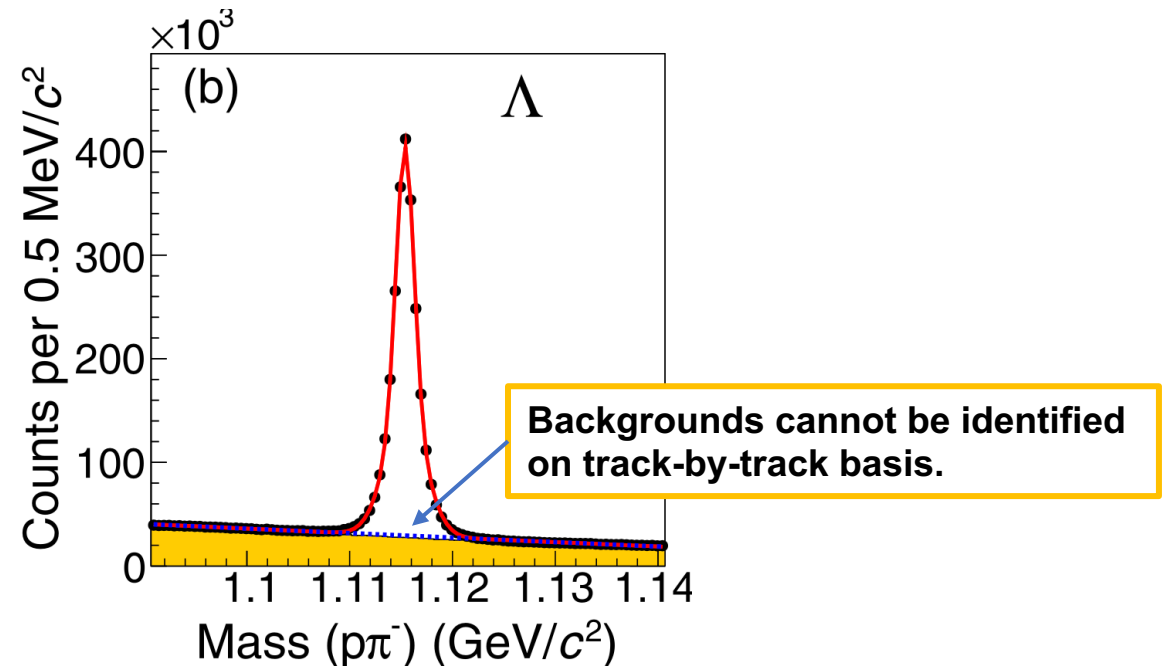
$$\begin{aligned} &-(\langle \Lambda \rangle_c + \langle \bar{\Lambda} \rangle_c) \\ &- 2(\langle \Xi^- \rangle_c + \langle \bar{\Xi}^+ \rangle_c) \end{aligned}$$

Analysis

Hyperon reconstruction



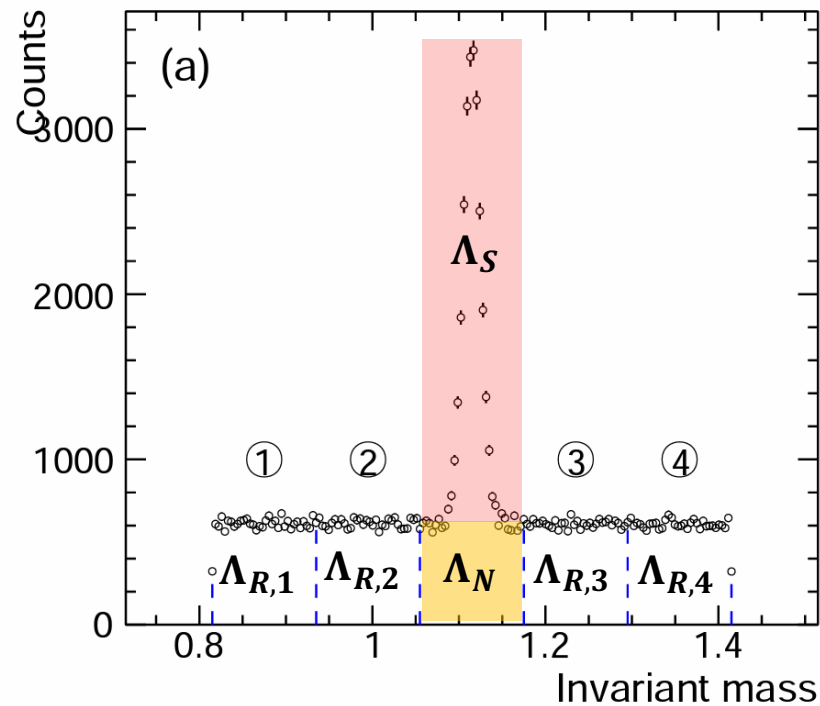
- Hyperons are reconstructed by using the invariant mass technique.
- The signal peak suffers from the combinatorial backgrounds depending on the cut conditions.



Purity correction: methodology

T. Nonaka, NIMA.1039.167171(2022)

We can only measure $\Lambda_{SN} = \Lambda_S + \Lambda_N$



- Λ_S and Λ_N cannot be obtained directly.

$$\Lambda_{SN} = \Lambda_S + \Lambda_N$$

$$\langle \Lambda_S^2 \rangle_c = \langle \Lambda_{SN}^2 \rangle_c - \langle \Lambda_N^2 \rangle_c - 2\langle \Lambda_S \Lambda_N \rangle_c$$

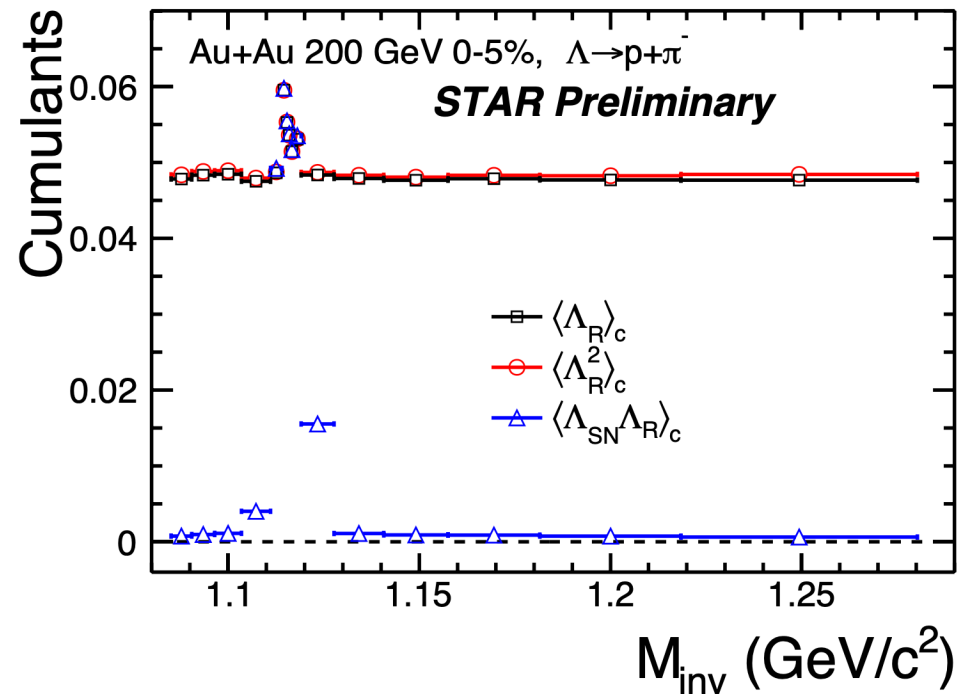
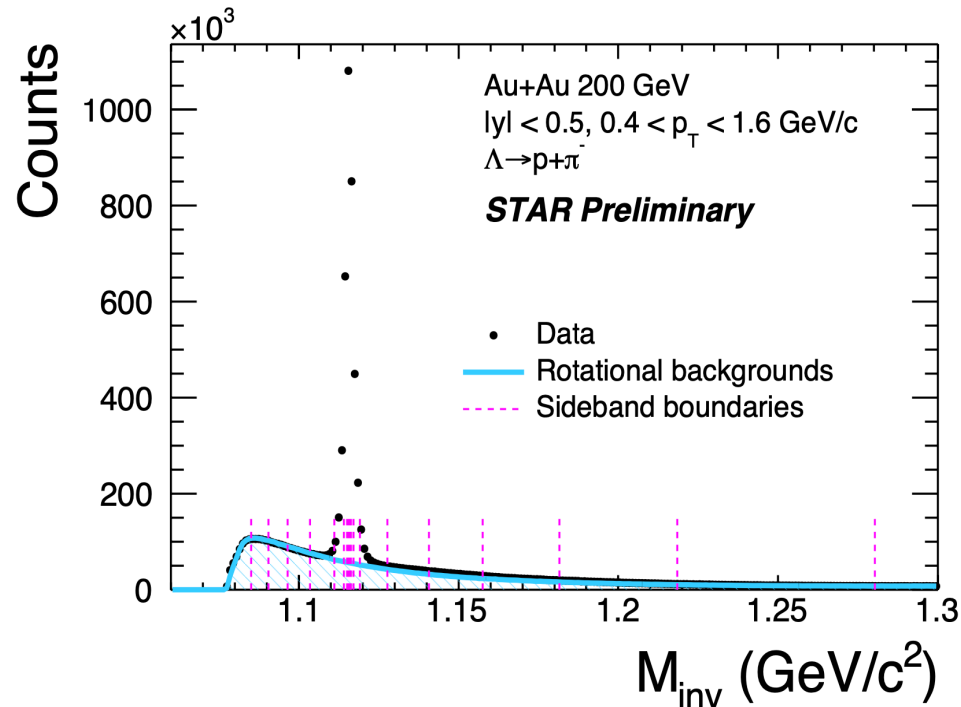
Assumption

Particle number distribution of the backgrounds under the signal peak is consistent with that in sideband.

$$\langle \Lambda_S^2 \rangle_c = \langle \Lambda_{SN}^2 \rangle_c - \langle \Lambda_{R,i}^2 \rangle_c - 2\langle \Lambda_{SN} \Lambda_{R,i} \rangle_c + 2\langle \Lambda_{R,i} \Lambda_{R,j} \rangle_c \quad (i \neq j)$$

Purity correction: sideband cumulants

- Sidebands are divided into small windows based on the yield of the signal candidates.
- Correction parameters are flat at sidebands, which can be used as a proxy of backgrounds under the signal peak.



Efficiency correction

- Efficiency correction is applied assuming the binomial response of efficiency.

$$B_{p,N}(n) = \frac{N!}{n!(N-n)!} p^n (1-p)^{N-n}$$

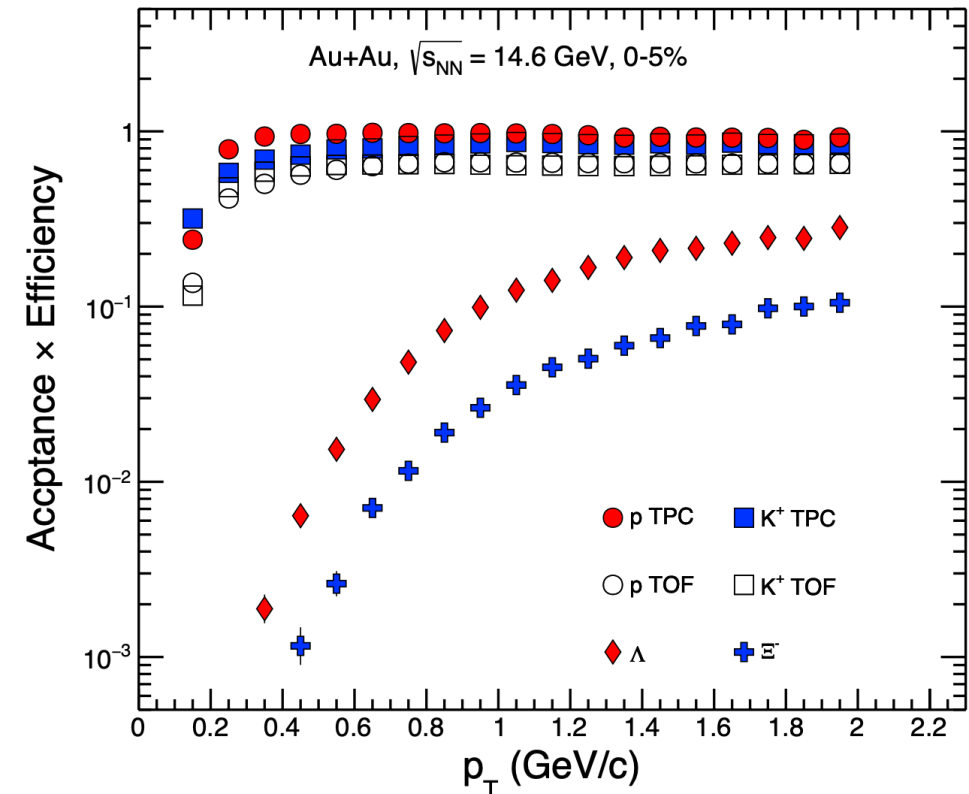
p : efficiency
 N : generated particles
 n : measured particles

T. Nonaka, M. Kitazawa, S. Esumi, PRC95.064912(2017)
X. Luo and T. Nonaka, PRC99.044917(2019)

$$\langle Q(x) Q(y) \rangle_c = \langle q(1,0,1) q(0,1,1) \rangle_c + \langle q(1,1,1) \rangle_c - \langle q(1,1,2) \rangle_c,$$

$$q(r,s,t) = q(x^r y^s / p^t) = \sum_{i=1}^M (x_i^r y_i^s / p_i^t) n_i.$$

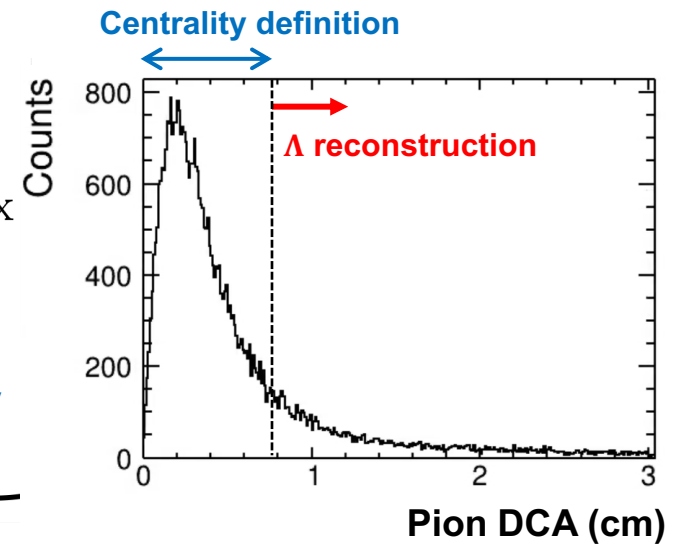
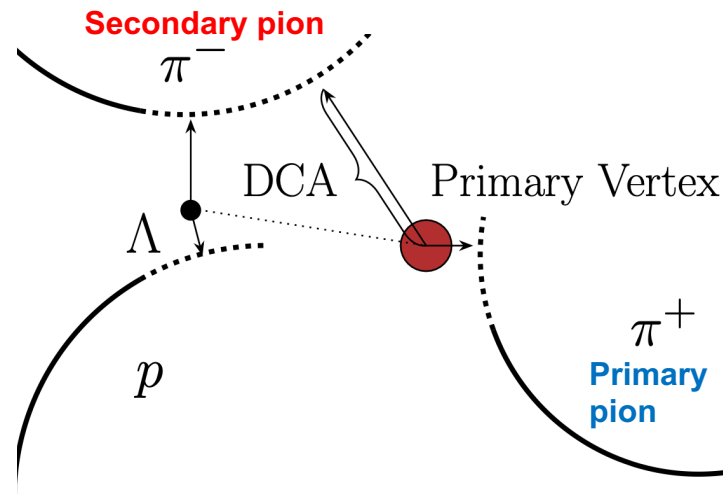
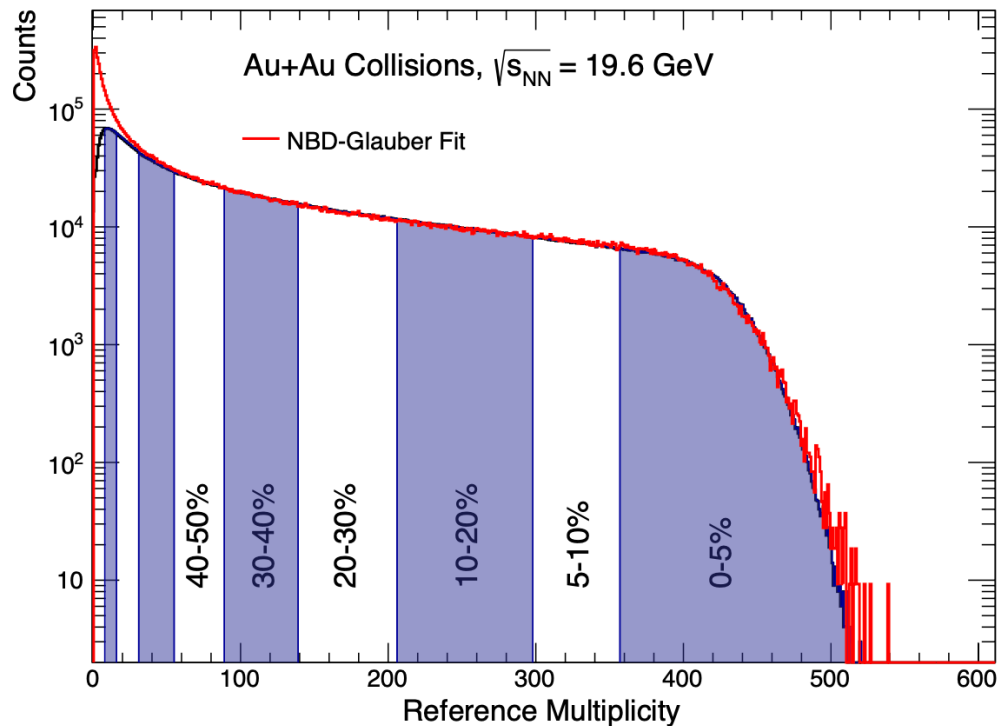
M : # of efficiency bins
 n : # of particles
 p : efficiency
 x, y : electric charge



Centrality definition

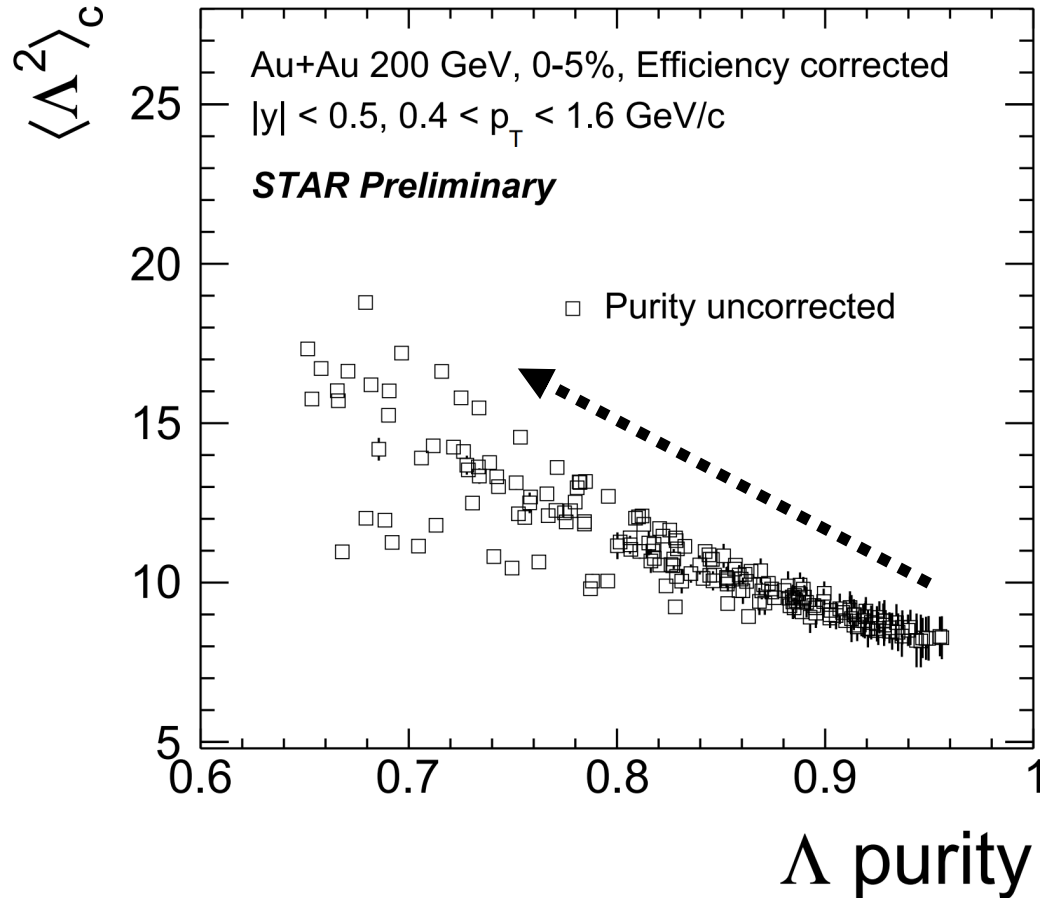
- The centrality is determined with π^\pm ($|\eta| < 1$) identified by TPC and TOF:

- Pions are used for Λ reconstruction by requiring large value of DCA.
- Pions having shorter DCA are used for the centrality definition.

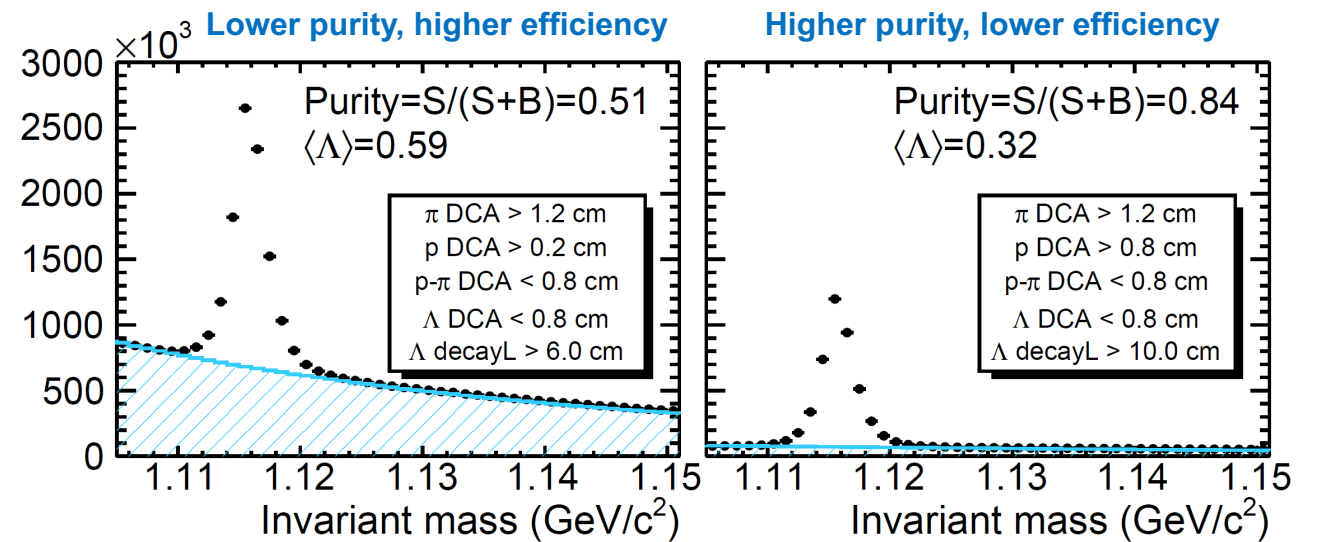


Results

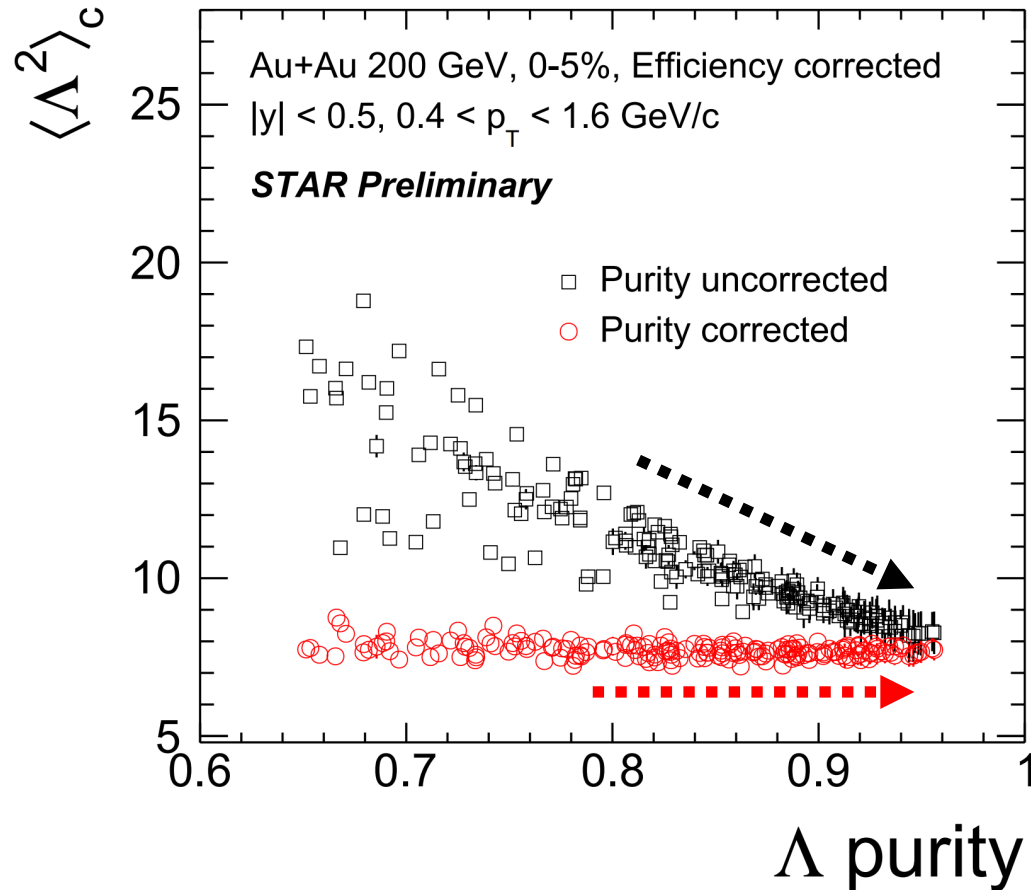
Purity correction: validation in STAR data



- The 2nd-order Λ cumulant is analyzed for **various topological cut sets having different purity/efficiency.**



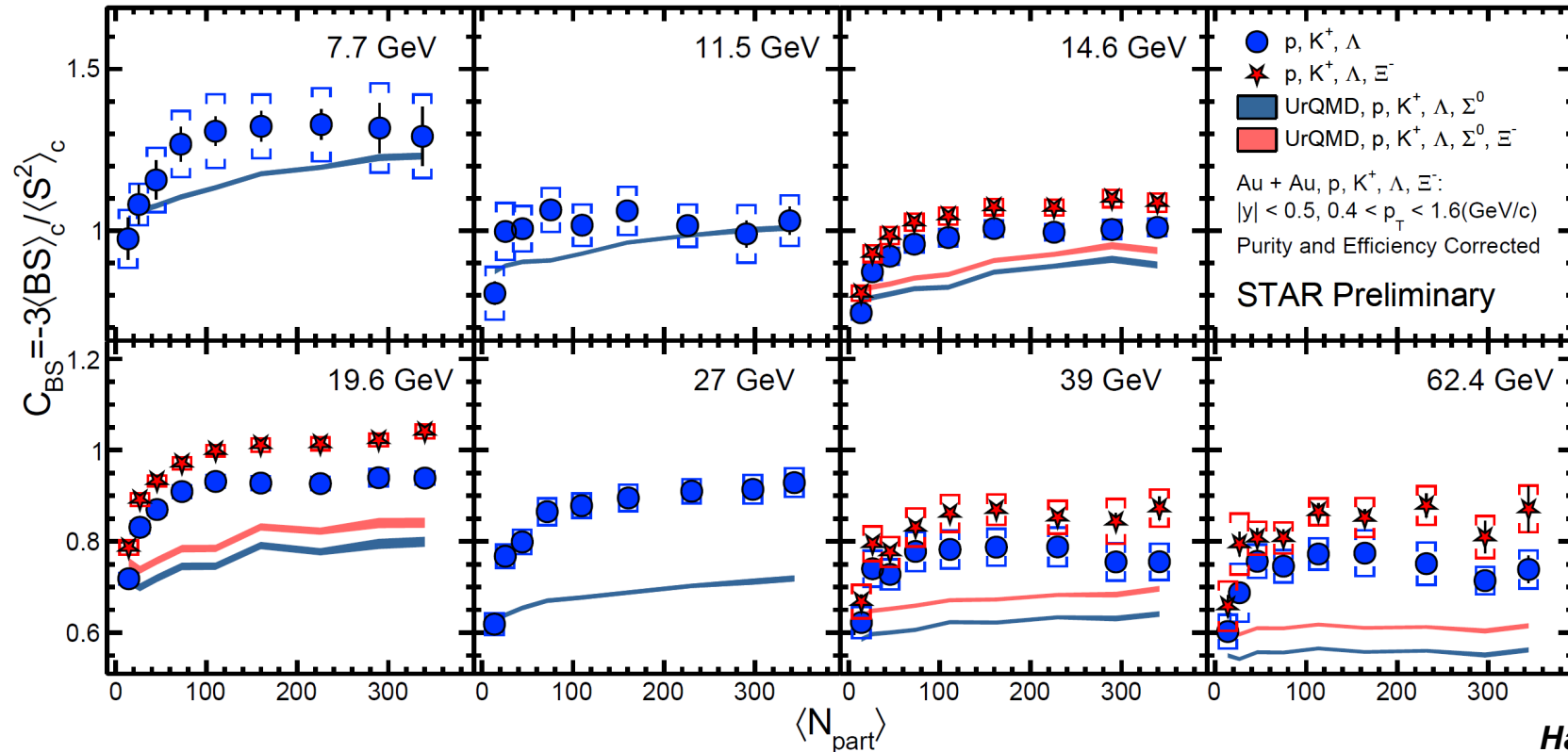
Purity correction: validation in STAR data



- The 2nd-order Λ cumulant is analyzed for **various topological cut sets having different purity/efficiency**.
- Purity/efficiency corrected cumulants are **flat and crosses with the uncorrected cumulants at the highest purity**, indicating the validity of the methodology.
- Residual variations are taken into account in systematic uncertainties.
- Statistical uncertainty can be minimized by tuning the cut sets, which will be critical for higher-order analysis.

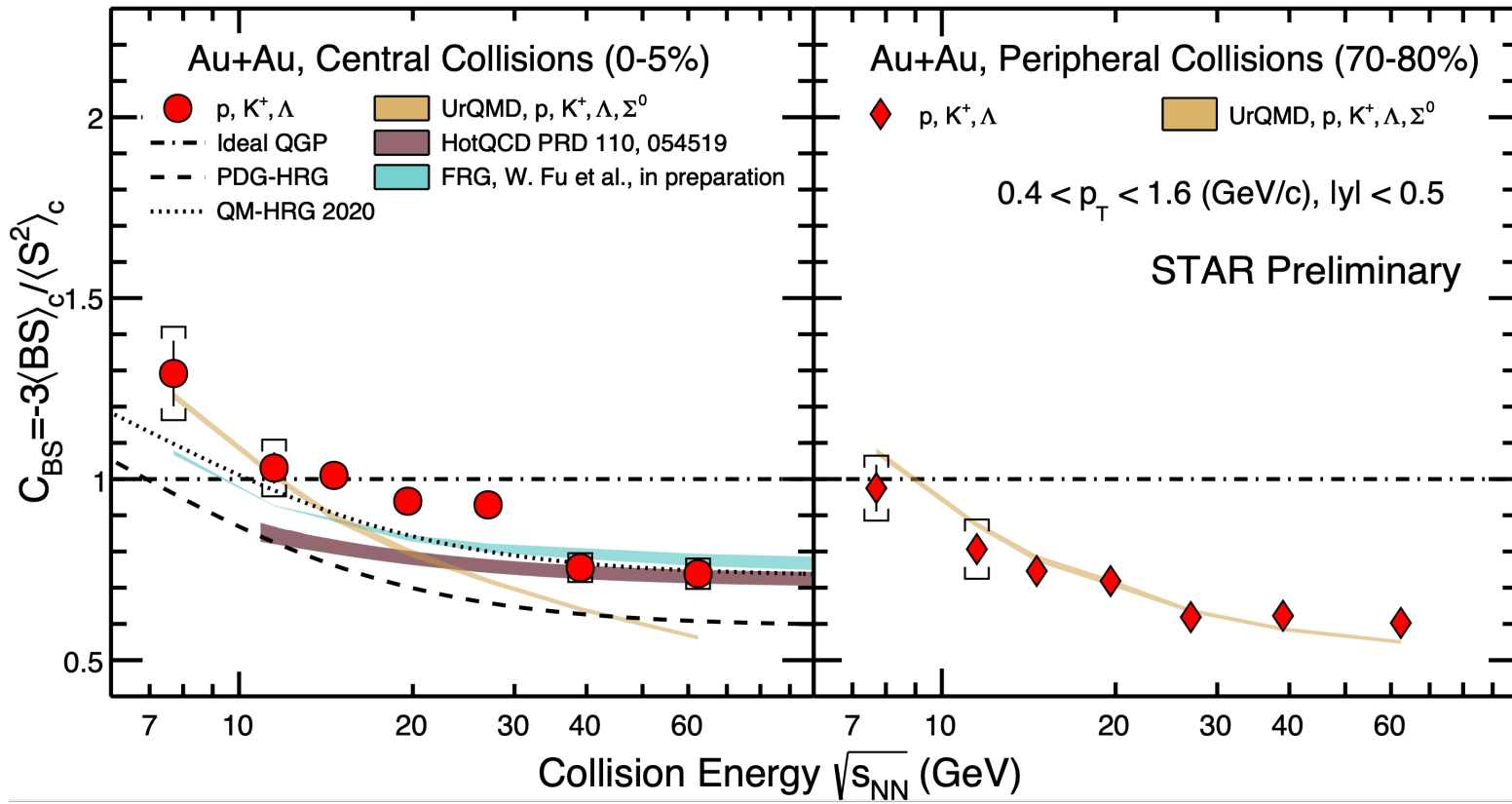
Centrality dependence

- Results are roughly reproduced by UrQMD at 7.7 and 11.5 GeV, while underestimated at higher energies.



Hanwen Feng, CPOD2024

Collision energy dependence



Central collisions

- Lower energies are reproduced by UrQMD, while higher energies are described by FRG and LQCD.
- Energy dependence is qualitatively reproduced by HRG calculations.

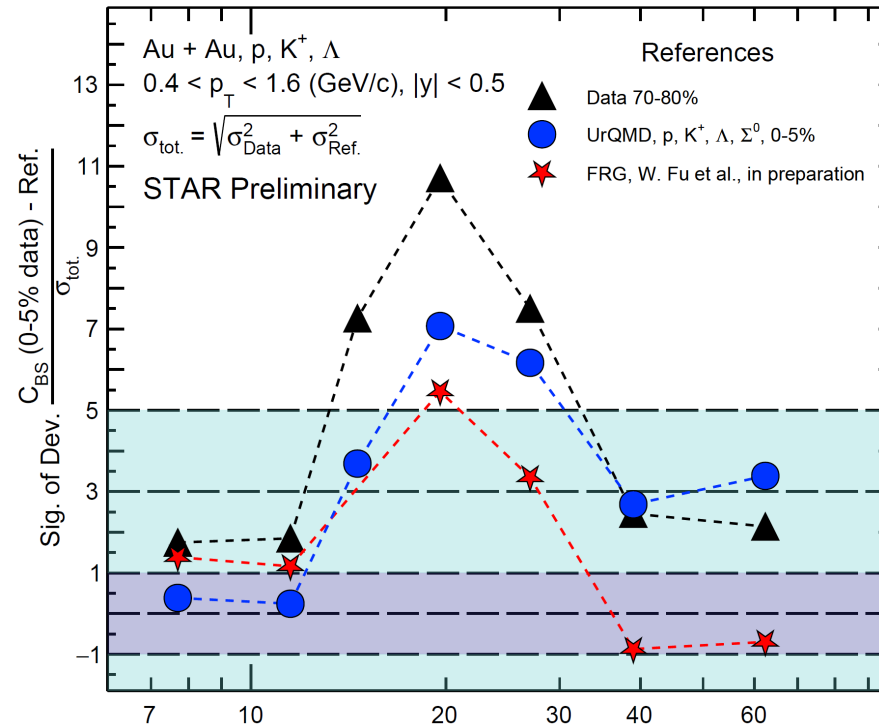
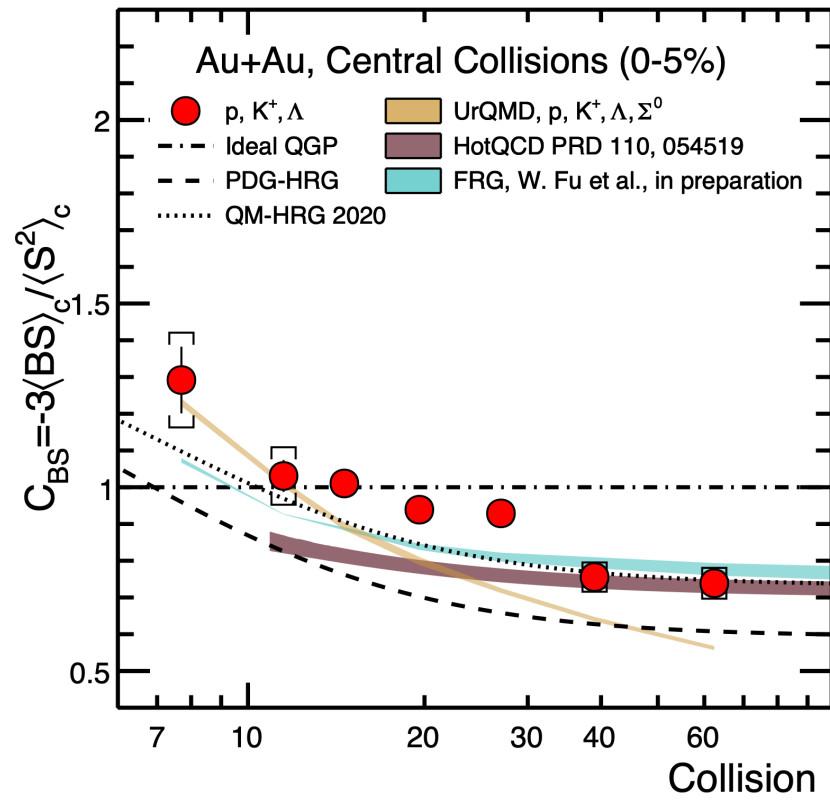
Peripheral collisions

- Well reproduced by UrQMD.

Hanwen Feng, CPOD2024

Comparison to model calculations

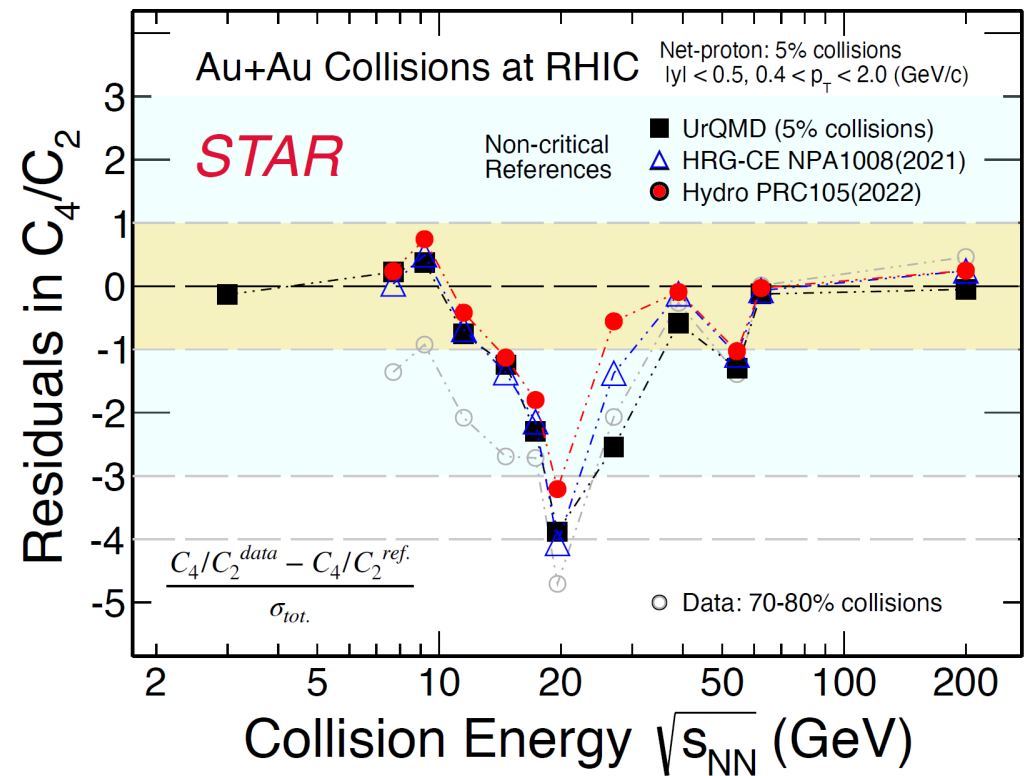
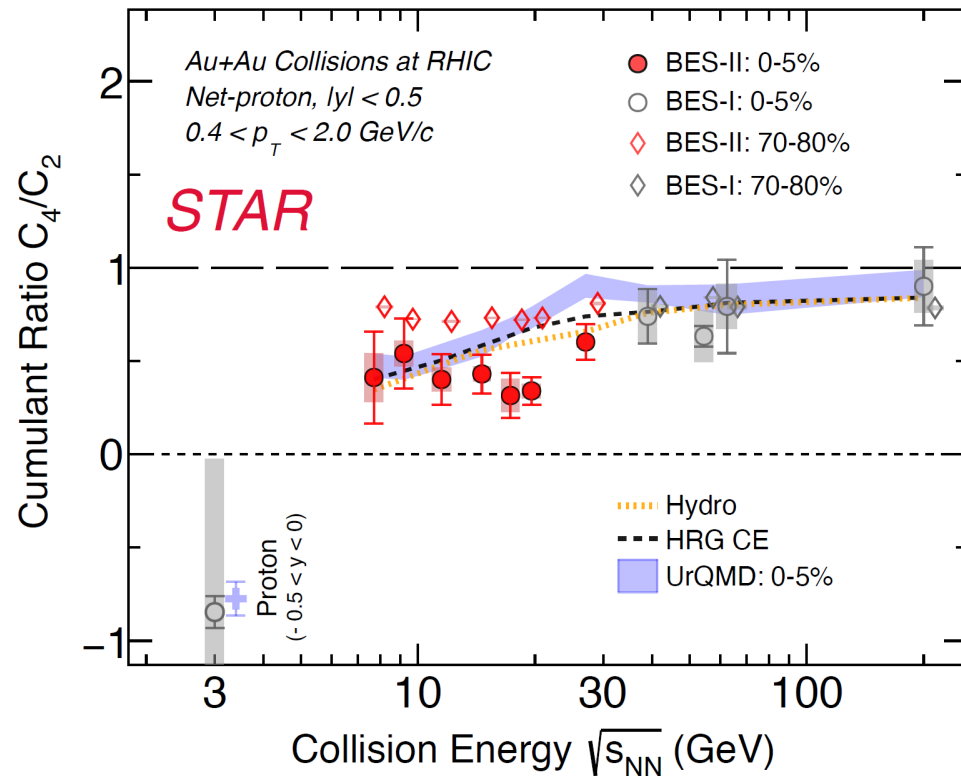
- The largest deviation (5-11 σ) is seen in ~20 GeV.



Hanwen Feng, CPOD2024

Similar to net-proton C_4/C_2 ...

Ashish Pandav, CPOD2024



C_4/C_2 shows minimum around ~ 20 GeV comparing to non-CP models, 70-80% data

Summary and outlook

- 2nd-order baryon-strangeness correlations have been measured including Λ and Ξ hyperons.
- Purity correction has been established to remove the effect of combinatorial backgrounds from hyperon number fluctuations.
- The values of baryon-strangeness correlations (C_{BS}) have been significantly enhanced compared to previous measurements without hyperons.
- Theoretical inputs are needed to interpret the largest deviation with model calculations at ~ 20 GeV.
- Analysis of BQ and QS correlations are ongoing for isobar data. Higher-order analysis will be also done in near future.

Thank you for your attention

Backup slides